Eur. Phys. J. Special Topics **146**, 407–425 (2007)
© EDP Sciences, Springer-Verlag 2007
DOI: 10.1140/epjst/e2007-00196-5

THE EUROPEAN PHYSICAL JOURNAL SPECIAL TOPICS

Pattern formation and localized structures in monoatomic layer deposition

M.G. Clerc[1,a], E. Tirapegui[1], and M. Trejo[2]

[1]Departamento de Física, Facultad de Ciencias Físicas y Matemáticas, Universidad de Chile, Casilla 487-3, Santiago, Chile
[2]Laboratoire de Physique Statistique, École Normale Supérieure, 24 rue Lhomond, 75231 Paris Cedex 05, France

Abstract. We study the nonlinear robust behaviors of a model for the deposition of a monolayer of molecules on a surface which takes into account the interactions of the adsorbed molecules. The transport properties of the model lead to non Fickian diffusion. It is shown that we have generically Turing structures coexisting with uniform concentrations and consequently localized structures through the pinning mechanism. The characteristic lengths are in the nanometer region in agreement with recent experiments.

1 Introduction

In the recent decades thin films used as electronic devices in industrial applications have become more and more complex. Due to this fact it is of great scientific and technological interest to understand and control the thin film growth, since growth mechanisms determine film mechanical, electrical, magnetic, and texture properties. The development of experimental methods, such as field ion microscopy or scanning tunneling microscopy, has opened up the possibility to monitor chemical reactions on the surface of metals in real time with an almost atomic resolution. The consequences of this microscopic reaction properties, which could previously could only be deduced through their influence on the global reaction rate or other macroscopic properties of a reaction, become now directly observable. Experiments have shown that absorbed molecules often form clusters or islands [1]. In the presence of reactions, non-equilibrium spatio temporal patterns with sizes lying in the nanometer range have been observed [2]. One has also observed nano patterns on solid surfaces [3–7], and nano structure islands in absorbed mono atomic layers [8]. These intriguing experimental observations have stimulated several theoretical and numerical studies. A promising strategy to describe this type of problem is the use of molecular dynamics simulations, however, this requires deposition rates which are unattainable. To simulate thin-film growth under more realistic deposition rates, a Monte Carlo approach has been developed. Unfortunately, the computational time required remains excessive. Indeed, a significant limitation of these methods is that they can deal only with small systems (micron). Hence, the continuous approach remains interesting, since it is able to modelize the growth of thin-films of larger sizes [9].

The aim of this manuscript is to show how the interplay between local kinetic processes and a simultaneously occurring phase transition, modelized by equations of the reaction diffusion type, may provide a suitable mechanism for the formation of localized structures with sizes lying in the nanometer range. We call these solutions *Nano localized structures*. In the case of

[a] e-mail: marcel@dfi.uchile.cl

a non linear kinetic processes, close to the spatial bifurcation we derive an adequate amplitude equation, which can explain the observed patterns.

The model that we consider takes into account both the kinetic exchange between the surface and the gas bathing, and also the thermodynamics of phase coexistence over the surface. Below a critical temperature T_c, lateral attractive interactions at long distance and repulsive at short distance between the absorbed molecules may induce a phase transition. To describe the kinetics of adsorption and activated desorption we introduce source terms in the mass balance equation. The local molecular coverage $c(\mathbf{r}, t)$ of the substrate $(0 \leq c \leq 1)$ satisfies the equation

$$\partial_t c = R[c] - \nabla \cdot \mathbf{J}, \tag{1}$$

where $\{R[c], \mathbf{J}\}$ represents the reaction terms and the mass current flow, respectively. Hence, if one has low coverage $c(\mathbf{r}, t) \ll 1$. The reaction rate has the expression $R[c] = k_{ad} P_s (1 - c) - k_{des} c^n$, where P is the pressure of the gas above the adsorbed layer, s is the sticking coefficient, k_{ad}, and k_{des} are the adsorption and desorption constant rates, respectively, and $n = \{1, 2\}$. This parameter gives account of the type of activated desorption processes considered: linear $(n = 1)$ or nonlinear $(n = 2)$. The adsorption and desorption rates are functions of the physical parameters involved in the deposition mechanism and according to the processing method, they may also depend on the coverage field $c(\vec{r}, t)$ [10]. However, for processing methods such as sputtering and laser assisted deposition (non equilibrium processes), in some temperature range the assumption of constant desorption rate independent of the coverage is fully justified [11]. The mass current flow satisfies

$$\mathbf{J} = -M \nabla \frac{\delta F}{\delta c},$$

where M is the surface mobility which is supposed to be constant, and $\mathcal{F}$ is the free energy of the adsorbed monolayer. An explicit expression for this free energy can be obtained as a correction of mean field theory [12] or from the microscopic lattice model with a metropolis algorithm for the probability transition in the limit of the local approximation (the radius of the interaction between the adsorbed particles is much shorter than all characteristic length scale of emerging structures) [10], and it may be written as

$$\mathcal{F}[c, \nabla c] = \int_s \left(k_B T f(c) - \frac{\varepsilon_o}{2} c^2 + \frac{\zeta_o^2}{2} |\nabla c|^2 \right) \mathrm{d}r, \tag{2}$$

where $k_B T$ is Boltzmann factor, and $f(c)$ a function to be defined in the next section together with the constants (ϵ_o, ζ_o).

Our objective then is to study in detail the model we have the deposition of a monolayer of molecules on a surface where they can move or react. We shall give in the appendix a short derivation of the model in the spirit of the work of Mikhailov [10] which shows its limits and possible generalizations. This description which involves partial differential equations of fields describing the deposition and the growth is able to explain the behavior at mesoscopic scales (from the order of nanometers to hundreds of nanometers), and plays then an intermediate role between the macoscopic and the microscopic behavior. We shall concentrate here in trying to give an appropriate description of the dynamics of a monolayer which can give us an understanding of the early behavior of the growth mechanism. Our analysis is done in the frame of reaction diffusion systems with non Fickian diffusion which we have recently studied generically [13].

In section 2, we present the reaction diffusion model which desorption and nonlinear diffusion of molecules in a substrate. In section 3 and section 4, we study the dynamics exhibited by the model for linear and nonlinear desorption rate, respectively. In section 5 we consider the case of very low or high coverage. In this situation the reaction terms can be treated as a perturbation of the transport term and the dynamics around the uniform coverage state can be approached by a a modified Cahn–Hilliard model [6]. In section 6, we give our conclusions.

2 Reaction diffusion model

The basic equation we shall use to describe the deposition of a mono layer of molecules in a surface where they can move or react, which is derived in the Appendix, is (see [10])

$$\partial_t c(\mathbf{r},t) = R[c(\mathbf{r},t)] + \nabla \cdot \left(D\nabla_c(\mathbf{r},t) - \frac{D}{k_B T} c(1-c)\nabla U(\mathbf{r}) \right), \tag{3}$$

which is of the type of equation (1) with the flux $\mathbf{J}[c(\mathbf{r},t)] = -(D\nabla c(\mathbf{r},t) - \frac{D}{k_B T} c(1-c)\nabla U(\mathbf{r}))$. The field $c(\mathbf{r},t)$, the local coverage, is defined as the quotient between the number of adsorbed molecules in a cell of the surface and the fixed number of available sites in each cell ($c(\mathbf{r},t) \leq 1$). The term $D\nabla^2 c$ in (3) is normal diffusion with coefficient D, k_B is Boltzmann constant, T the temperature and the last term represents the flow of the adsorbed molecules which move under the force given by the gradient of the potential $U(\mathbf{r})$ produced in that point by the other molecules. The factor $(1-c)$ takes care of the fact that the flow can only pass through the available vacant sites in each cell (*a finite occupancy effect*) and the potential can be written as $U(\mathbf{r}) = -\int u(\mathbf{r}-\mathbf{r}')c(\mathbf{r}')\mathrm{d}\mathbf{r}'$ where the function $u(\mathbf{r})$ is a spherically symmetric interaction potential between molecules separated by a distance $|\mathbf{r}|$. When the interaction radius is small compared to the diffusion length and the covering $c(\mathbf{r},t)$ does not vary significantly within the interaction radius, we can approximate the integral by $\epsilon_o c(\mathbf{r}) + \zeta_o^2 \nabla^2 c(\mathbf{r})$ with $\epsilon_o = \int u(\mathbf{r})\mathrm{d}\mathbf{r}, \zeta_o^2 = \frac{1}{2}\int |\mathbf{r}|^2 u(\mathbf{r})\mathrm{d}\mathbf{r}$, and we have used $\int \mathbf{r}u(\mathbf{r})\mathrm{d}\mathbf{r} = 0$ due to symmetry.

The flux $\mathbf{J}[c(\mathbf{r},t)]$ in equation (3) is proportional to the conjugate thermodynamic force which arises from the spatial variation of the associated chemical potential $\varphi[c(\mathbf{r},\mathbf{t})]$, i.e we can write $\mathbf{J}[c(\mathbf{r},t)] = -M(c)\nabla\varphi[c(\mathbf{r},t)]$, where $M(c) = Dc(1-c)/k_B T$ is the mobility and φ will be the functional derivate of a *free energy* $\mathcal{F}\varphi[c(\mathbf{r},t)] = \delta f[c(\mathbf{r})]/\delta c(\mathbf{r})$. Equation (3) can then be written in the form

$$\partial_t c(\mathbf{r},t) = R[c(\mathbf{r},t)] + \nabla \cdot \left[M(\mathbf{c}(r,t)\nabla \frac{\delta \mathcal{F}[c(\mathbf{r})]}{\delta c(\mathbf{r})} \right], \tag{4}$$

with $f(c) = (1-c)\ln(1-c) + c\ln(c)$.

The reaction rate has the expression $R[c] = \alpha_o(1-c) - \beta_o c^n$, We shall further simplify our model taking a constant mobility $M(c) = M_o$ independent of $c(\mathbf{r},t)$, this will not change the qualitative dynamics of the model which is our interest here. The equations are then

$$\partial_t c = \alpha_o(1-c) - \beta_o c^n + M_o \nabla^2 \varphi, \tag{5}$$

$$\varphi = -\epsilon_o c + k_B T \ln\left[\frac{c}{1-c}\right] - \zeta_o^2 \nabla^2 c. \tag{6}$$

We recall that stationary states and their linear stability have been studied in a similar model with constant or exponential dependence of desorption rate, for $n = 1$ [12,14,15], and for $n = 2$ [11].

It is important to remark that the model (5) has a Lypunov functional for the linear case ($n = 1$):

$$F = \int \left[K_B T f(\mathbf{r}) - \tfrac{1}{2}\epsilon_o c(\mathbf{r})^{\mathbf{2}} + \tfrac{\mathbf{1}}{\mathbf{2}}\zeta_{\mathbf{o}}^{\mathbf{2}} |\nabla \mathbf{c}(\mathbf{r})|^{\mathbf{2}} \right] \mathrm{d}\mathbf{r} + \frac{\alpha_o}{M} \int G(\mathbf{r},\mathbf{r}')c(\mathbf{r})\,\mathrm{d}\mathbf{r}'\mathrm{d}\mathbf{r}$$
$$+ \frac{\alpha_o + \beta_o}{2M} \int c(\mathbf{r})G(\mathbf{r},\mathbf{r}')c(\mathbf{r}')\,\mathrm{d}\mathbf{r}'\mathrm{d}\mathbf{r}. \tag{7}$$

where G is the *Green Function* defined by the *Poisson* equation, $\nabla^2 G(\mathbf{r},\mathbf{r}') = -\delta(\mathbf{r}-\mathbf{r}')$, with boundaryconditions vanishing at infinity. In two and one dimensions this function takes the form

$$G(\mathbf{r},\mathbf{r}') = -\frac{1}{2\pi}\ln|\mathbf{r}-\mathbf{r}'|; \qquad G(\mathbf{r},\mathbf{r}') = \frac{|\mathbf{r}-\mathbf{r}'|}{2},$$

respectively, and therefore the system can be written as:

$$\partial_t c(\mathbf{r},t) = M\nabla^2 \frac{\delta F}{\delta c(\mathbf{r})}. \tag{8}$$

The first terms of the free energy correspond to an attractive short range interaction given by the parameters $\{\zeta_o, \epsilon_o\}$, and the two last terms of the free energy represent the nonlocal effective repulsive short range interaction governed by absorption and desorption processes. Hence, the dynamics of model (5) in the linear case is characterize by the minimization of the free energy (7), that is, the dynamics exhibited by the above model is of relaxation type.

If one neglects the absorption and the desorption processes, the model (5) becomes a Cahn-Hilliard type equation. This model is characterized by exhibiting a phase transition at a critical temperature $T_c = \epsilon_0/4K$, that is, for $T > T_c$, the uniform coverage states are stable and they are unstable for $T < T_c$, giving rise to a region of high coverage surrounded by a region of low coverage, and viceversa. This scenarios changes drastically when the absorption and the desorption processes are taken into account.

3 Dynamics of the monolayer for linear desorption ($n = 1$)

3.1 Pattern formation in the weakly non linear regime

In the case of linear desorption, the above model only exhibits one uniform coverage state: $c_o = k/s(1+k)$, with $k \equiv \alpha_o/\beta_o$, When the value of this homogeneous concentration c_o is moderate ($0.3 \sim c_o \sim 0.7$), we analyze the equation for small perturbations around c_o. Replacing $c(\mathbf{r},t) = c_o + \sigma(\mathbf{r},t)$ in the equation (5), we find for $\sigma(\mathbf{r},t) \ll 1$:

$$\partial_t \sigma(\mathbf{r},t) = -\Omega\sigma + \Gamma\nabla^2 \left[-\sigma(\mathbf{r},t) + \mu \ln\left(\frac{c_o + \sigma(\mathbf{r},t)}{1 - c_o - \sigma(\mathbf{r},t)} \right) - \nabla^2\sigma(\mathbf{r},t) \right], \tag{9}$$

where $\Gamma = D_o\epsilon_o^2/\zeta_o^2 K_B T = M_o\epsilon_o^2/\zeta_o^2$, and $\Omega = \alpha_o + \beta_o, \mu = T/4T_c$. Moreover, we can introduce the spatial and temporal scaling $X = \sqrt{\epsilon_o/\zeta_o^2}x$ and $\tau = \Gamma t$, these scalings normalize the adsorption and desorption constant rates. The temporal scaling is equivalent to take units so that $\Gamma = 1$. To analyze the linear stability we use the ansatz $\sigma(\mathbf{r},t) = A_o e^{\lambda t + ikx}$. Replacing this expression in the equation (9), we obtain the relation

$$\lambda(k) = -\Omega - \epsilon\Gamma k^2 - \Gamma k^4; \tag{10}$$

where $\epsilon = -1 + \mu/c_o(1-c_o)$. If we fix the values of deposition rates ($\{\alpha_o, \beta_o\}$), then the only free parameter is the temperature T. Therefore, for certain value $T < T_P \equiv 4T_c c_o(1-c_o)[1 - k_p^2 - \Omega/k_p^2\Gamma]$($k_p = \sqrt[4]{\Omega/\Gamma}$, and $T_p < T_c$) the homogeneous solution becomes unstable and gives rise to an spatially periodic state, whose wavelength is of the same order of the wavelength of the unstable mode of the uniform coverage state. In figure 1, we show the spectrum $\lambda(k)$for different temperature values and fixed deposition rates. Hence, the uniform coverage state c_o is stable for $T > T_P$. Note that, for $T > T_c$ the coefficient of the diffusion term of model (5) is positives and becomes negatives in the interval $T_p < T < T_c$. In this parameter region, the long range interactions dominate the system and the perturbations of the uniform coverage state are characterized by hyper-diffusive dynamical behaviors.

Close to the spatial instability, one can use the standard weakly nonlinear analysis (amplitude equation), the system shows patterns with sizes lying in the nanometer range [14]. In this reference the bifuraction diagram of pattern formation is determined close to the spatial instability and it is shown that this bifurcation is of the supercritical type, that is, close to the instability there appears a pattern with small amplitude (proportional to the square root of the bifurcation parameter). In 2D, close to threshold, the system exhibits stripes or hexagons parameters values.

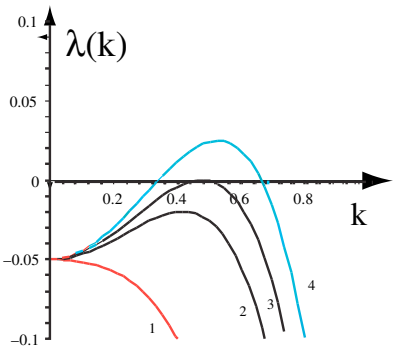

Fig. 1. Spectrum $\Lambda(k)$ for different values of temperature. Diffusive regime (curve 1, $\epsilon = 0.37$), hyperdiffusive (curve 2, $\epsilon = -0.12$), marginal regime (curve 3, $\epsilon = 0.22$), and onset of instability (curve 4. $\epsilon = -0.32$).

Throughout the previous analysis the only free parameter has been the temperature. In experiments the deposition is an isothermal process, and in this case the reduced gaseous phase above the adsorbed layer is the only externally tunable parameter, producing simultaneously the variation in the adsorption rate $\alpha_o = k_{ad}P_s$. This description has been considered in [11], and involves only a quantitative change of the scheme presented above.

3.2 Pattern formation and localized structures in the highly nonlinear regime

When the value of the homogeneous concentration is not moderated ($c_o < 0.3$ or $c_o > 0.7$), the numerical simulations of equation (9) show that the spatial instability now is characterized by large amplitude. The region in the parameter space in which these patterns are obseryed is very small. The typical pattern coverage state observed in this regime is depicted in figure 2 for 1D. In this parameters region an interesting phenomenon can be observed. Nearby to the bifurcation point, pattern formation with large amplitude takes places (cf. figure 2), that is, to the bifurcation point, pattern formation with large amplitude takes places (cf. figure 2) that is, a pattern coverage state and uniform coverage states are stable and coexist in a narrow region

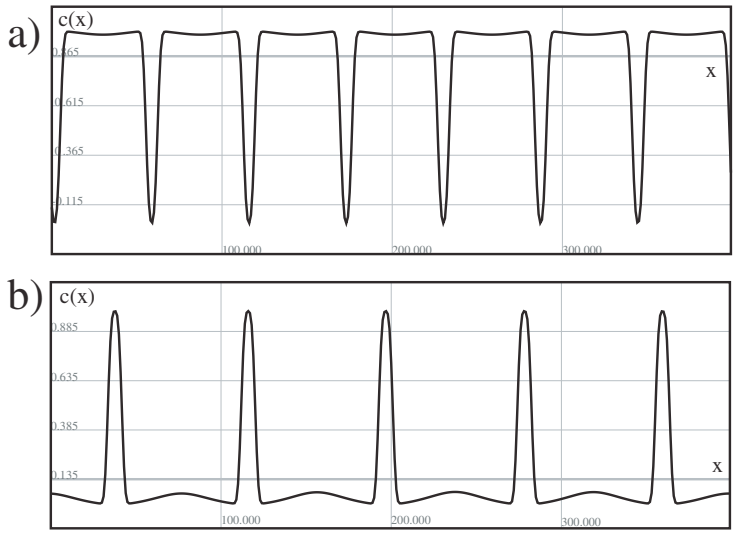

Fig. 2. Pattern coverage stage in one dimensional model (9). (a) Numerical simulation of highly nonlinear pattern in one dimensional model (9) with high coverage for: $c_o = 0.865$, $\mu = 0.1$, $\Omega = 0.005$, $\Gamma = 1$, $k_{ad} = 0.004325$, $k_{des} = 0.000675$, $\sigma_{min} = -0.842$, $\sigma_{max} = 0.126$. (b) Numerical simulation of highly nonlinear pattern in one dimensional model (9) with low coverage for: $c_o = 0.135$, $\mu = 0.1$, $\Omega = 0.005$, $\Gamma = 1$, $k_ad = 0.004325$, $k_{des} = 0.000675$, $\sigma_{min} = -0.126$, $\sigma_{max} = 0.857$.

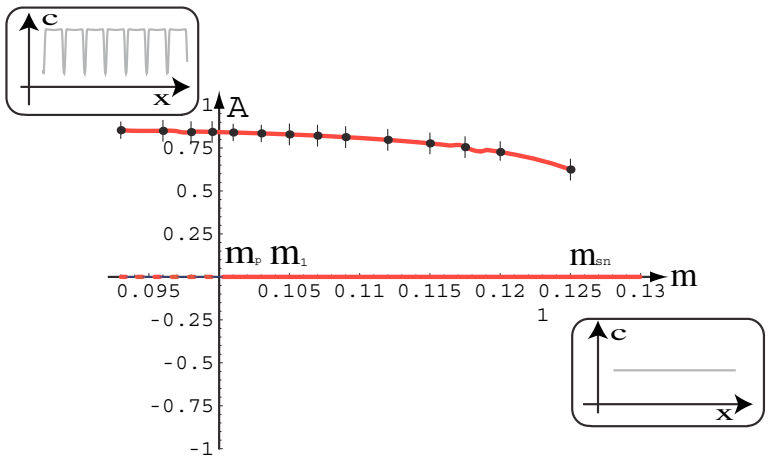

Fig. 3. Bifurcation diagram for $n = 1$. When $\mu_1 = 0.1014$ the pattern one propagates on the state homogeneous. In $\mu_p = 0.10026$ appear the periodical soultions by saddle node bifurcation. The inset figures stand for the respective coverage states.

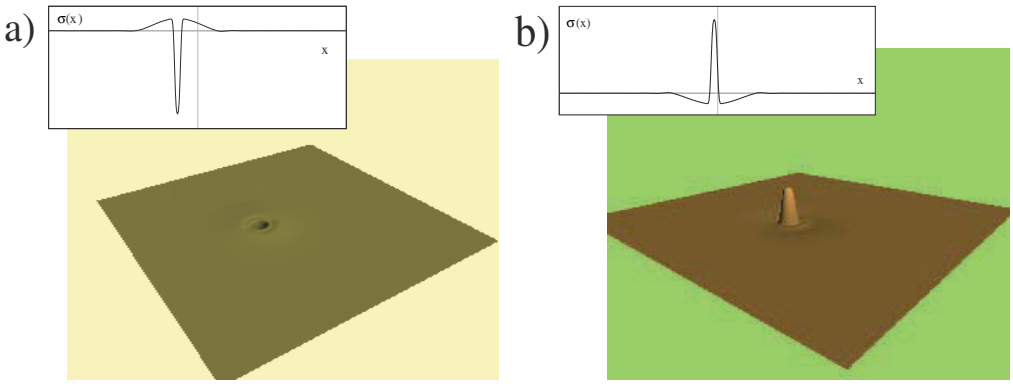

Fig. 4. Localized structures (adsorption and desorption island) in one and two dimensional system. This structures are formed in the Pinning region in the highly nonlinear regime. a) Numerical simulation of equation (9) in one and two dimensional system. We see the localized structures formation (Desorption island) for: $\mu = 0.105, c_o = 0.865, \omega = 0.005, \Gamma = 1, \beta = 0.004325, \alpha = 0.000675$. In the inset figure we have: $\sigma_{min} = -0.846, \sigma_{max} = 0.119$. b) Numerical simulation of equation (9) in one and two dimensional system. We see the localized structures formation (Adsorption island) for: $\mu = 0.105, c_o = 0.1355, \Omega = 0.005, \Gamma = 1, \alpha = 0.004325, \beta = 0.000675$. In the inset figure we have: $\sigma_{min} = -0.119, \sigma_{max} = -0.845$.

of parameter space. In figure 3, we show the bifurcation diagram, that is, the amplitude A of the steady state coverage pattern observed in the one dimensional model (5) as function of μ. This bifurcation is characterized by two critical points, the bifurcation point $\mu_p = T/4T_p$ (point in the parameter space where the uniform coverage states becomes unstable) and the bistablity point μ_{sn} (point in the parameter space where the pattern state appears by saddle-node bifurcation). Between these two points the system exhibits coexistence between these coverage states. Note that in general, it is a difficult task to find μ_{sn}. as function of the physical parameters. Inside of this parameter region, we observed localized pattern and nano localized structures in one and two spatial dimensions. In figure 4, we present the typical localized coverage patterns observed in this model. One can understand these localized structures as patterns extended only over a small portion of an extended system. From the point of view of dynamical systems theory, these solutions in 1D are homoclinic connections of the spatial dynamical system [16,17].

Since in this regime the value of the homogeneous states c_o are far from the critical value $c_c = 0.5$, the highest orders in the logarithm expansion are important and one can not derive

an amplitude equation and a bifurcation diagram, because the numerical simulations show that the patterns have large amplitude and are far from being harmonic solutions, on the contrary the interfaces are sharp. When two coverage states coexists (pattern and uniform coverage states), we can expect the appearance of fronts, that is, dynamical solutions of equation (9), which connect spatially the two states. These fronts move with a characteristic speed and the favorable state (energetically) invades the unfavorable one. Recently, it has been demonstrated geometrically [17] and also by means of an amplitude equation [16], that these fronts are motionless in a range of parameters, the *pinning range*. It is important to remark that this region contains the Maxwell point, where both states are energetically equivalent. Outside this region the front propagates. The localized patterns are observed close to the pinning range. In figure 4, we show the typical localized coverage structure formed at the pinning region. We can see the weak oscillation in the edge of the structure. From the values of the parameters used in the simulations we can estimate the typical size of the localized coverage structure and we and that it is $d \approx 8\,\mathrm{nm}$.

4 Dynamics of the monolayer for nonlinear desorption $(n = 2)$

When we consider more complex processes for the desorption like chemical reactions between the deposited atoms and the substrate or collisions processes between themselves (for instance a diatomic desorption process) [11], we must include nonlinear reaction terms in the equation (3), i.e. $n = 2$. As we shall see the inclusion of this term will modify the above bifurcation diagram scenarios. In particular, the system will exhibit localized coverage structure and patterns with small amplitude.

4.1 Linear stability analysis and extended pattern formation

The equation which describes the system reads

$$\partial_t c(\mathbf{r},t) = \alpha_o[1 - c(\mathbf{r},t)] - \beta_o c(\mathbf{r},t)^2 + M_o\nabla^2\left[-\epsilon_o c(\mathbf{r},t) + K_B T \ln\left[\frac{c(\mathbf{r},t)}{1-c(\mathbf{r},t)}\right] - \xi_o^2\nabla^2 c(\mathbf{r},t)\right]. \tag{11}$$

For nonlinear desorption, the system has two uniform coverage states, only one with physical sense ($c_o \leq 1$)

$$c_o = \frac{\alpha_o}{2\beta_o}\left(\sqrt{1 + \frac{4\beta_o}{\alpha_o}} - 1\right). \tag{12}$$

The equation for the small perturbation $\sigma(\mathbf{r},t)$ to this solution is then:

$$\partial_t\sigma(\mathbf{r},t) = -\alpha\,\sigma - \beta_o\sigma^2 + \Gamma\,\nabla^2\left[-\sigma(\mathbf{r},t) + \mu\ln\left(\frac{c_o + \sigma(\mathbf{r},t)}{1 - c_o - \sigma(\mathbf{r},t)}\right) - \nabla^2\sigma(\mathbf{r},t)\right]. \tag{13}$$

The last term, which represents the transport in equation (13), remains inalterable (μ and Γ are exactly the same that the case $n = 1$). $\alpha \equiv \alpha_o\sqrt{1 + 4\beta_o/\alpha_o}$ is the reduced adsorption cofficient. In order to describe analytically the onset of the spatial instability, we linearize the above model, we use the ansatz $\sigma = \sigma_o e^{\lambda(k)t + ikx}$, and we obtain the following dispersion relation

$$\lambda(k) = -\alpha - \epsilon\Gamma k^2 - \Gamma k^4. \tag{14}$$

Note that the only change with respect to the linear case $n = 1$ is the α coefficient instead of Ω in equation (10). Therefore, in this system the pattern formation takes place in a weak segregation regime [11]. The critical value of temperature for when the uniform coverage becomes spatially unstable is

$$T_p = 4T_c c_o(1 - c_o)\left[1 - k^2 - \frac{\alpha}{k^2\Gamma}\right], \tag{15}$$

where $k_p = \sqrt[4]{\alpha/\Gamma}$. The above expression can be written as $T_p = 4T_c(1-|\epsilon_p|)c_o(1-c_o)$, with $|\epsilon_p| = T_p/4T_c = 2\sqrt{\alpha/\Gamma}$. When the temperature decreases under a critical value ($T < T_p$), a spatially modulated perturbation with wave number close to the critical wave number begins to grow generating an extended pattern coverage state [11]. In this reference, one can found the typical competition between hexagons and stripes patterns. Note that the same dynamical behavior was found in the linear adsorption [12].

4.2 Localized patterns in the weakly nonlinear regime

For values of the uniform coverage c_o close to the critical concentration ($c_c = 0.5$), we shall see that it is possible to find localized patterns in the weakly nonlinear regime. The oscillations of these patterns will be smooth and with moderated amplitude, therefore, we can make an analytical description by means of amplitude equations (weakly nonlinear analysis). The quadratic term associated with the nonlinear desorption process plays an important role in the dynamics of the monolayer, because it is able to change the type of bifurcation.

In order to describe the dynamics of the monolayer we expand the equation (13) up to the fifth order in σ

$$\begin{aligned}\partial_t\sigma(\mathbf{r},t) = &-\alpha\,\sigma(\mathbf{r},t) - \beta_o\sigma(\mathbf{r},t)^2 + \Gamma\,\nabla^2[\epsilon\sigma(\mathbf{r},t) + \omega\,\sigma(\mathbf{r},t)^2 + \theta\,\sigma(|bfr,t)^3 + \gamma\,\sigma(\mathbf{r},t)^4 \\ &+ \delta\,\sigma(\mathbf{r},t)^5 + \cdots - \nabla^2\sigma(\mathbf{r},t)],\end{aligned} \tag{16}$$

We can write this equation around the bifurcation, $\epsilon = -(|\epsilon_p|+v), v > 0,\ v \ll 1$, and separating the linear and nonlinear terms, we have

$$\partial_t\sigma = \mathcal{L}[\sigma] + NL[\sigma], \tag{17}$$

were $\mathcal{L}$ is the operator of the linear part. In one dimension it has the form

$$\mathcal{L} = -\alpha + \epsilon\Gamma\,\partial_{xx} - \Gamma\,\partial_{xxxx}, \tag{18}$$

The nonlinear part $NL[\sigma]$ correspond to the logarithm expansion in power series. To describe analytically the localized solutions observed in one dimensional extended systems close to the spatial instability, we use the ansatz (the nonlinear change of variables)

$$\sigma(x,t) = A(\tau \equiv vt, y \equiv v^{1/2}x)e^{ik_px} + \text{c.c} + \cdots + W, \tag{19}$$

where A is the amplitude of the spatially oscillatory solution, k_p is the critical wave-number ($k_p = 2\pi/\lambda_p$), and $W$is a small correction function. Rewriting in a more suggestive form

$$\sigma(x,t) = \sigma^{[1]} + \sigma^{[2]} + \sigma^{[3]} + \cdots \tag{20}$$

where $\sigma^{[i]}$ indicates order i in the power of A in the change of variables, that is, $\sigma^{[1]} = A(\tau,y)e^{ik_px} + \text{c.c}$, $\sigma^{[2]} = a_1A^2e^{2ik_px} + \overline{a}_1\overline{A^2}e^{-2ik_px} + a_2\,|A|^2$ and so forth. Replacing (19) in the equation (16) and linearizing in W one obtains the following solvability equation for the linear part

$$v\partial_\tau A = k_p^2 v\,\Gamma A + 4v\Gamma\,\partial_{yy}A, \tag{21}$$

This equation is given by the terms proportional to the critical mode e^{ik_px} (the *resonant term*). Note that at the following order we have

$$\partial_t\sigma^{[2]} = 0, \tag{22}$$

and therefore, replacing the change of variable to order 2, we have for the same powers of A

$$-\mathcal{L}\sigma^{[2]} = NL\{\sigma^{[1]}\}^{(2)}, \tag{23}$$

where the {} bracket in the right hand side of the equation (23) stands for quadratic terms. This last equation allows us to find the coefficients a_1,$\overline{a_1}$,a_2, as function of the physical parameters. In this calculation the spatial derivatives on A are of order v and therefore they are negligible. We obtain

$$a_1 = \overline{a_1} = \frac{-\beta_o - 4\Gamma\,\omega\,k_p^2}{\alpha + 4 \in \Gamma\,\kappa_p^2 + 16k_p^4\Gamma}; \qquad a_2 = \frac{-2\beta_o}{\alpha}, \tag{24}$$

Iterative application of this method, allow us to obtain all the coefficients of the change of variables as function of the previous order according to

$$-\mathcal{L}\sigma^{[s]} = NL[\sigma^{[s-1]}]^{(s)}. \tag{25}$$

Then, introducing the ansatz in equation (5) and linearizing in W, we obtain the following solvability condition:

$$\partial_t A = c_1 A + c_3\,|A|^2\,A + c_5\,|A|^4\,A + \mathcal{D}\partial_{xx}A + \text{h.o.t.}, \tag{26}$$

where h.o.t stands for the resonant higher order terms and $c_1 = v\,|\epsilon_0|/2$ is the bifurcation parameter. Hence, when c_1 is positive the system exhibits pattern formation. The parameter c_3 bifurcation (super or sub critical bifurcation depending on the sign of this coefficient, for $c_3 > 0$ the bifurcation is super-critical), $\mathcal{D}$ is the effective diffusion for the amplitude A, and if $c_5 < 0$ and $c_3 \ll 1$, using the scaling $A \sim \sqrt[4]{c_1}, \partial_t \sim c_1, c_3 \sim \sqrt{c_1}, c_5 \sim \mathcal{D} \sim O(1)$, and $\partial_x \sim \sqrt{c_1}$, we can neglect the higher order terms. The full (and lengthy) expressions of these coefficients $\{c_3, c_5, \mathcal{D}\}$, as a function of their physical parameters, has been determined by standard *normal form* techniques [18]. In figure 5, we exhibit the values of the coefficients as functions of the uniform coverage state. In the region of parameters of the subcritical bifurcation (cf. gray region of figure 5) the above amplitude equation (26) exhibits coexistence between the uniform state ($A = 0$) and the pattern coverage state ($A = \sqrt{\left|c_3 + \sqrt{c_3^2 - 4c_1c_5}\right|}/2\,|c_5|$). However, the resonant amplitude equation (26) does not exhibit localized structures because these solutions are a consequence of the interaction of the large scale envelope (A) with the small scale underlying the spatially periodic solution, contained in the non resonant terms [16] . This conjecture has been corroborated in [19] for the case of a particular example in a one dimensional system. To describe the localized structure, and explain the *Locking phenomena* where the fronts are stationary, we consider the *amended amplitude equation* with the dominant non resonant terms (or non adiabatic terms):

$$\partial_t A = c_1 A + c_3\,|A|^2\,A + c_5\,|A|^4\,A + \mathcal{D}\partial_{xx}A + (m_1\,|A|^2\,A^2 + m_2 A^4)e^{ik_c x/\sqrt{c_1}}, \tag{27}$$

where $\{m_1, m_2\}$ are complex number and depend on the physical parameters. Notice that the non resonant terms play the role of a spatial parametric forcing with rapidly varying oscillations and these terms restore the discrete spatial invariance of the amplitude ($x \to x + x_o$, $A \to Ae^{ik_c x_o}$), and also that if we have considered an additive noise (which is generically present in a macroscopic equation) in the original equation this would add to the previous equation a term proportional to $e^{-ik_c x/\sqrt{c_1}}\xi(x,t)$, with $\xi(x,t)$ a $\delta-$ *correlated* white noise in time and

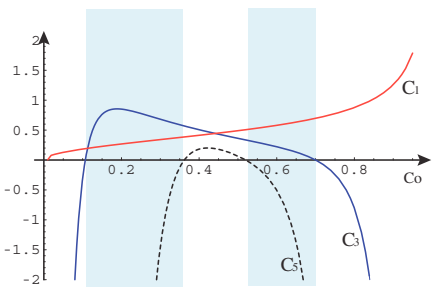

Fig. 5. Cofficients of the amplitude equation (26) as function of the uniform coverage state c_0. The other physical parameters have been fixed to $\Gamma = 1$, $\mu = 0.0092$, and $\beta = 0.16$.

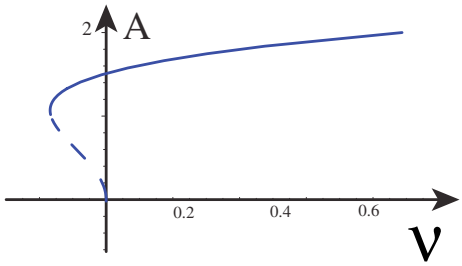

Fig. 6. Subcritical bifurcation diagram for the system in the weakly nonlinear system for the same parameters that in figure 7.

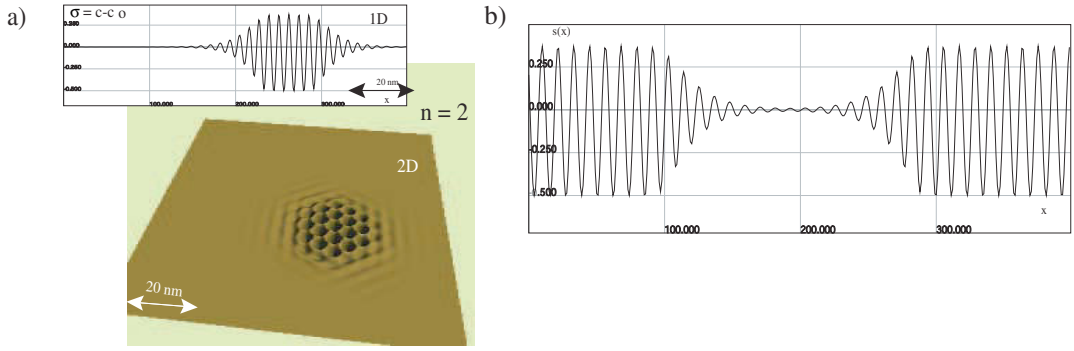

Fig. 7. Localized pattern in one and two dimensional system. Numerical simulations of equation (11) for: $\mu = 0.0092$; $c_o = 0.5$; $\alpha_o = 0.008$; $\beta_o = 0.16$, $\Gamma = 1$. In addition we have for the inset figure $\sigma_{min} = -0 - 49916$, $\sigma_{max} = 0.370704$, $\sigma = c - c_o$. a) Localized pattern and b) hole solution.

space (if the original noise had this property) which will give by itself the same effect as the previous non resonant terms and moreover will in general be dominant near the bifurcation point [16,20,21].

In figure 6, we show the subcritical bifurcation which exhibits the coexistence between two coverage states, for the parameters in which we have observed the localized patterns formation numerically. The resonant amplitude equation has analytical solutions for a front which links the uniform to the spatially periodical coverage states, and this solution is the starting point to calculate the front interaction. Due to the oscillatory nature of the front interaction, which alternates between attractive and repulsive, we infer the existence, stability properties, dynamical evolution and bifurcation diagram of localized patterns. These localized structures are a consequence of *the pinning effect or Locking phenomena*, as it can be seen in an alike amended amplitude equation deduced from a prototype model of pattern formation [16]. Inside the pinning range, we observe localized patterns in one and two spatial dimensions. In figure 7, we present the typical localized patterns observed in the model (4). One can understand these localized structures as patterns extended only over a small portion of an extended system. Moreover the existence of these localized structure can be proved rigourously in 1D using the tools of dynamical systems theory in the spatial dynamical system [17].

In figure 7, we show the numerical simulation of equation (13) in the range of parameters where the bifurcation is subcritical and that has been predicted by the calculations. Here, we can see the smallest structure that can be formed figure 7(a). In figure 7(b), we can see a localized pattern, in which the supported state is a pattern coverage state, that is, this state is a uniform state surround by a pattern one. This state is usually called *Hole solution*.

4.3 Pattern formation and localized structures in the highly nonlinear regime

At the onset of the spatial bifurcation of the uniform coverage state for large and small coverage ($c_o < 0.3$ or $c_o > 0.7$), the numerical simulation of the equation (13) shows pattern formation of large amplitude, such as in the linear desorption case (cf. figure 8). Again, we expect to find in

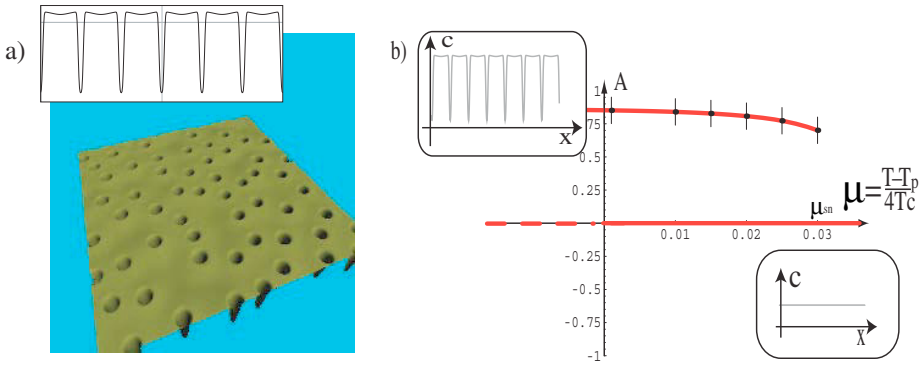

Fig. 8. Pattern formation in the highly nonlinear regime and numerical Bifurcation diagram. a) Numerical bifurcation diagram in the highly nonlinear regime for $c_o = 0.86264, \alpha_o = 0.005, \alpha_o = 0.00379, \beta_o = 0.0007, \Gamma = 1$. We can see that the structures formation happens in the hysteresis zone. b) Numerical simulation of (13) in one (inset of figure) and two dimensional system. Pattern formation in the highly nonlinear regime for $\mu = 0.1, \alpha = 0.005, \alpha_o = 0.00379, \beta_o = 0.0007, c_o = 0.8626$. The amplitude is $\sigma_{min} = -0.85116$.

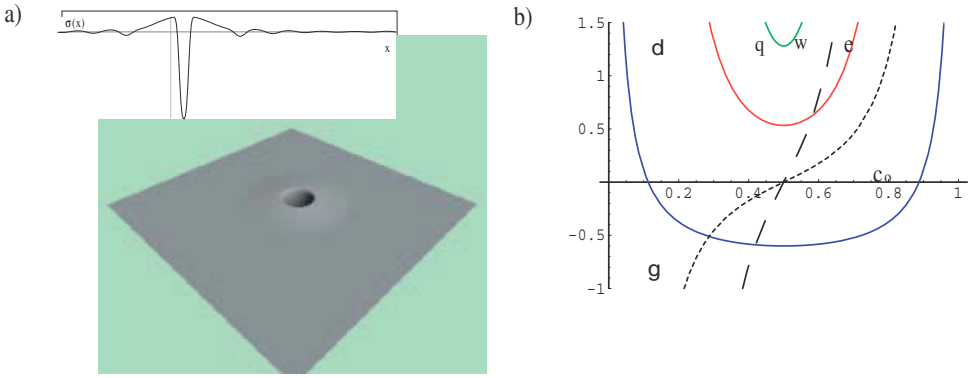

Fig. 9. Localized structures formation by the Pinning mechanism in the coexistence zone. a) Vacancy island in two dimensional system for the equation (13) and b) Coefficients in the logarithmic expansion.

a certain region of the parameter space the coexistence between high amplitude patterns with states of uniform coverage. In this zone of parameters, we expect to find localized structures with different numbers of oscillations. The localized structure with a single oscillation will be termed *vacancy island* (*adsorption island*) in the case of high (low) value of the uniform coverage c_o. In figure 9 a vacancy island is displayed in this region

In brief, in the coexistence zone of coverage states, we observe the localized structure for mation by means of the *pinning mechanism*, that is, these solution are consequence of the front interaction. In figure 8(a), we show the amplitude A of the steady state as function of the bifurcation parameter μ. This bifurcation is characterized by two critical points, the bifurcation point $\mu_p = T/4T_p$ (cf. figure 8(a)), and the bistablity point μ_{sn} (point in the parameter space where the pattern coverage state appears by saddle-node bifurcation). Between these two points, the system exhibits a coexistence between uniform and spatially periodic coverage states (hysteresis region). Close to this parameter region, we observe localized pattern in one and two spatial dimensions.

4.4 Two patterns states coexistence and Localized peaks

The equation (16) allowed us to have a region where the bifurcation was subcritical and the coexistence between homogeneous and patterns states was possible. Nevertheless, it is

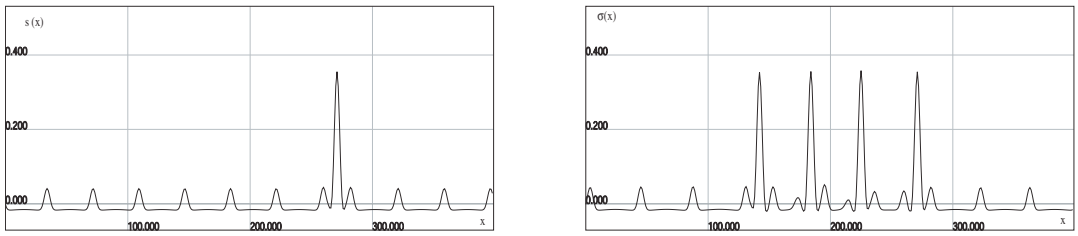

Fig. 10. Numerical simulation of equation (16) show us localized peaks formation for: $\mu = 0.0126; c_o = 0.0208; \alpha_o = 0.008, \beta_o = 0.19; \alpha_o = 8.4 \times 10^{-}5$. The values of amplitudes are: $\sigma_A = 0.35$ and $\sigma_B = 0.04$.

reasonable to take into account more terms in the expansion of equation (16) if we consider extremely low or high values for the uniform coverage c_o. One has an initial spatial super critical bifurcation, followed by a secondary subcritical bifurcation, that is, a *super-sub-critical bifurcation*. Hence, the system can exhibit coexistence of two spatially coverage periodic states. Recently in reference [22], by means of amended amplitude equation it has been shown that a bi-pattern system generically exhibits *localized peaks*. This state appears as a large amplitude peak nucleating over a pattern of lower amplitude. Localized states are pinned over a lattice spontaneously generated by the system itself. Numerical simulations of model (13) in the bi-pattern region exhibits localized peaks, in figure 10, we show these type of coverage states in 1D. In figure 11(a), we show the bifurcation diagram obtained numerically for this bi-pattern region, where each branch represents a pattern coverage state. It is important to remark that in this case it is not possible to make analytical calculations similar to those done in [22], since the interfaces of the coverage state are sharp and the highly nonlinear terms in the equation (11) are very important, therefore weakly non linear analysis do not apply. However, the qualitative behavior and the underlying non linear analysis obtained in the non linear case leads the dynamics.

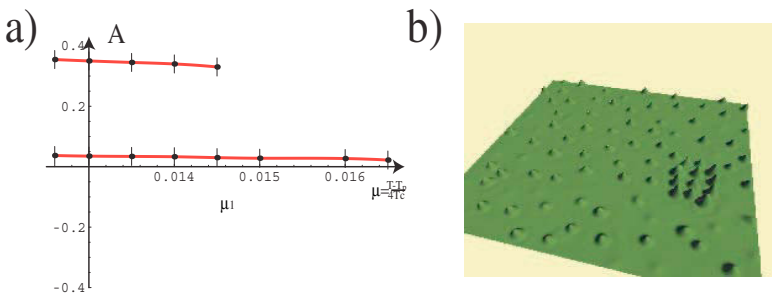

Fig. 11. Localized peaks and bifurcation diagram. a) Numerical bifurcation diagram in the coexistence zone for the same values that figure (10). In $\mu_1 = 0.015$ takes place the birth of greater amplitude pattern. b)Numerical simulation of equation (11)in two dimensional system for: $\mu_1 = 0.0126, c_o = 0.0208; \beta_o = 0.19, \alpha_o = 8.4 \times 10^{-}5$.

5 The perturbed Cahn–Hilliard limit and nano-structures like bubble

In the previous sections, we have found Localized structures (adsorption and desorption islands) in the highly non linear regime for linear ($n = 1$) and nonlinear desorption ($n = 2$) due to the coexistence between pattern and homogeneous states within the *Pinning region*. In this same region $\epsilon < 0$, the dynamical behavior of the system is of the hyper-diffusive type (See figure (1)) and the long range interaction dominate the dynamics. The competition between reaction and transport terms is at the origin of the patterns and localized structure formation in all previous regimes. The uniform coverage concentration *co* for this same parameter region is in the following interval

$$\frac{1}{2}\left[1-\sqrt{1-\frac{T}{T_c}}\right] < c < \frac{1}{2}\left[1-\frac{T}{T_c}\right]. \tag{28}$$

When c_o is outside of the interval (28), that is, the case of very low or high coverage, which is observed for small desorption rate ($\Omega \approx 10^{-4,}\, \alpha_o,\, \beta_o \ll 1$) the system is diffiusive ($\epsilon < 0$, see figure 1 or figure 9(b) and short range interaction are important. The reaction terms can be treated like a perturbation to the transport terms in the model (5) and the dynamics around the uniform coverage state can be approached by a modified Cahn-Hilliard model [13]. It is well known that the Cahn–Hilliard model exhibits a family of localized solutions, *bubbles solution* [23], and we will study the persistence of these solutions in this modified Cahn–Hilliard equation.

5.1 Nano-structures like bubble

The starting point is the equation (16), close to the bifurcation point the equation reads for small σ

$$\partial_t\sigma(\mathbf{r},t) = \alpha_o[1-c_o-\sigma] - \beta_o(c_o+\sigma)^2 + M_o\epsilon_o\nabla^2\left[\epsilon\sigma(\mathbf{r}) + \omega\,\sigma(\mathbf{r})^2 + \theta\,\sigma(\mathbf{r})^3\cdots + \frac{\xi_o^2}{\epsilon_o}\nabla^2\sigma(\mathbf{r})\right], \tag{29}$$

where the coefficients of the logarithm expansion in the transport terms are given by:

$$\mu\ln\left[\frac{c_o+\sigma}{1-c_o-\sigma}\right] = \ln\left[\frac{c_o}{1-c_o}\right] + \sum_{m=1}^{\infty} g_m(\mu,c_o)\sigma(\mathbf{r})^m,$$

with

$$g_m(\mu,c_o) = \frac{\mu}{m}\left[\frac{c_o^m-(c_o-1)^m}{c_o^m(1-c_o)^m}\right],$$

here $\epsilon = -1+g_1$, $\omega = g_2$, $\theta = g_3$, $g_4 = \gamma$, $g_5 = \delta$. Figure 9(b) shows the five coefficient for fixed temperature ($\mu = 0.1$) as function of the uniform coverage state c_o. We see that the odd coefficients are always positive and the segmented lines are the even coefficients. The linear coefficient ϵ is positive in a large region of uniform concentrations when $\mu < 0.25$. For very small reaction terms, the concentrations are in the range $c_o \sim 0.1$ or $c_o \sim 0.9$ and therefore $\epsilon > 0$.

In order to describe and understand the dynamics exhibited by the system, we model it by a perturbed Cahn–Hilliard equation. Therefore, we shall consider up to the cubic term in the expansion. We make a translation $\sigma = u - u_o$, in order to eliminate the quadratic term (ω) in equation (29). Finally, we scale the space and time variables and the system is modeled by

$$\partial_\tau u(y,\tau) = A + Bu + Cu^2 + \nabla^2[\tilde{\epsilon}u + u^3 - \nabla^2 u], \tag{30}$$

where $X = \xi/\sqrt{\epsilon_o}\theta x, \tau = \tilde{\Gamma}t, \tilde{\Gamma} = \Gamma\theta^2, \tilde{\epsilon} = \epsilon/\theta - 3u_o^2$, and $u_o = \omega/3\theta$. The value of this coefficient is small, since the coefficients of the logarithm expansion are large. On the other hand, the values of the coefficients A, B, and C depend on the type of desorption. For $n = 1$ we have:

$$A = \frac{\Omega}{\tilde{\Gamma}}u_o; \quad B = -\frac{\Omega}{\tilde{\Gamma}}; \quad C = 0, \tag{31}$$

and for quadratic desorption ($n = 2$) :

$$A = \frac{1}{\tilde{\Gamma}}(\alpha u_o - \beta_o u_o^2); \quad B = \frac{1}{\tilde{\Gamma}}(-\alpha + 2\beta_o u_o); \tag{32}$$

$$C = -\frac{\beta_o}{\tilde{\Gamma}}, \tag{33}$$

The coefficients of expression (31, 32, 33) are small in this range of c_o. Numerical simulations of the equation (9) and (13) show the appearance of localized structures for linear and nonlinear desorption process ($n = 1, 2$).

In the case of exclusively transport process ($A = B = C = 0$), the model (30) becomes the Cahn–Hilliard equation [24]. This model has been initially proposed to describe the phase separation dynamics in conservative system, such as binary alloys, binary liquids, glasses, polymer solutions, to mention a few. In the last decades the above model has been used to describe zig-zag instability undergone by straight rolls in two-dimensional extended systems like Rayleigh-Bénard convection or electroconvection in fluid systems (see review [29] and references therein). A similar zig-zag instability affecting anisotropic interfaces has been described in terms of this model [25–28]. It is worthy to note that the dynamical behaviors of the one-dimensional Cahn–Hilliard is well understood [27,28]. In [27] it is shown that Cahn–Hilliard equation has a bubble solution from two fronts interaction (Kink and Anti-Kink interaction), which has the form

$$U(x, x_\pm(t)) = -\sqrt{|\tilde{\epsilon}|} - \sqrt{|\tilde{\epsilon}|}\tanh\left[\sqrt{\frac{|\tilde{\epsilon}|}{2}}(x - x_-(t))\right] + \sqrt{|\tilde{\epsilon}|}\tanh\left[\sqrt{\frac{|\tilde{\epsilon}|}{2}}(x - x_+(t))\right] + \omega, \tag{34}$$

where $x_\pm = x_o \pm \Delta/2$ and ω is a small correction function of order $\mathcal{O}(\sqrt{|\tilde{\epsilon}|}e^{-\sqrt{2|\tilde{\epsilon}|\Delta}})$. Here $\{x_-(t), x_+(t)\}$ stand for the position of core of the kink and anti-kink, respectively. $\nabla(t) \equiv x_- - x_+$ is the width of the bubble, and $x_o(t)$ is the position of the bubble center. The above bubble correspond to a localized structure of low coverage when adsorption and desorption process have been neglected. To describe the nano-localized coverage pattern like bubble, when small reaction processes are take into account, we shall study the persistence of the bubble solution (34) when $c_o \leq 0.1$ (or $c_o \geq 0.9$).

Then, replacing ansatz (34) in equation (30) and linearizing in ω, we obtain

$$\mathcal{L}\omega = \partial_{z_-} u_- \dot{x}_- + \partial_{z_+} u_+ \dot{x}_+ A + B\rho + C\rho^2 + \partial_{xx}[\tilde{\epsilon}\rho + \rho^3 - \partial_{xx}\rho], \tag{35}$$

where $\mathcal{L}$ is a linear operator which has the form $\mathcal{L} \equiv \tilde{\epsilon}\partial_{xx} + 3\partial_{xx}(\rho^2) - \partial_{xxxx}, \rho$ is an auxiliary function defined as $\rho \equiv u_-\left[z_- \equiv \sqrt{|\tilde{\epsilon}|/2(x - x_-)}\right] + u_+\left[z_+ \equiv \sqrt{|\tilde{\epsilon}|/2(x - x_+)}\right] - \sqrt{|\tilde{\epsilon}|}, u_\pm \equiv \pm\sqrt{|\tilde{\epsilon}|\tanh[\sqrt{|\tilde{\epsilon}|}/2(x - x_\pm)]}$ are the kink and anti-kink solutions respectively, $x_\pm$ stand for the position of the core of the kink and anti-kink, respectively. Note that the above equation can write as $\mathcal{L}\omega = b$. Hence, in order to have solution, we should imposes the Fredholm alternative, that is, ω has solution if b is orthogonal to the elements of the kernel of the adjoint of $\mathcal{L}$ $b \perp v$, where $v \epsilon Ker(\mathcal{L}^\dagger)$ then b is in the image of $\mathcal{L}(b\,\epsilon\, Im(\mathcal{L}))$. Let us introduce the inner product $\langle f|\, g\rangle = 1/L\int_{-L/2}^{L/2} fg\,\mathrm{d}x$, where L is the system size. So, $\mathcal{L}^\dagger$ has the form $\mathcal{L}^\dagger = \tilde{\epsilon}\partial_{xx} + 3\rho^2\partial_{xx} - \partial_{xxxx}$. A base of $Ker(\mathcal{L}^\dagger)$ is $\{1, x, \int u_+\mathrm{d}x,\ \int u_-\mathrm{d}x\}$. Applying the solvability condition (Fredholm alternative) for the constant function, we obtain

$$d\dot{\Delta} = AL + 2B\sqrt{\tilde{\epsilon}}\Delta - B\sqrt{\tilde{\epsilon}}L + CL\tilde{\epsilon} - C\Delta\tilde{\epsilon}, \tag{36}$$

where $d = \pm\langle 1|\, \partial_{z_\pm} u_\pm\rangle$. The above equation describes the kink and anti-kink interaction. Then the equilibrium point must be $\dot{\Delta} = 0$ and we obtain finally the expression for the width of the localized solution of the perturbed Cahn–Hilliard model

$$\Delta_{eq} = -\frac{(A - B\sqrt{\tilde{\epsilon}} + C\tilde{\epsilon})}{2B\sqrt{\tilde{\epsilon}} - C\tilde{\epsilon}}L. \tag{37}$$

It is easy to verify that this equilibrium state is stable, i.e. the bubble solution is an attractor of equation model (36). It is worth to remark that in this extreme limit the localized coverage states depends on the size of the system and when $L \to \infty$ the system does not exhibit nano

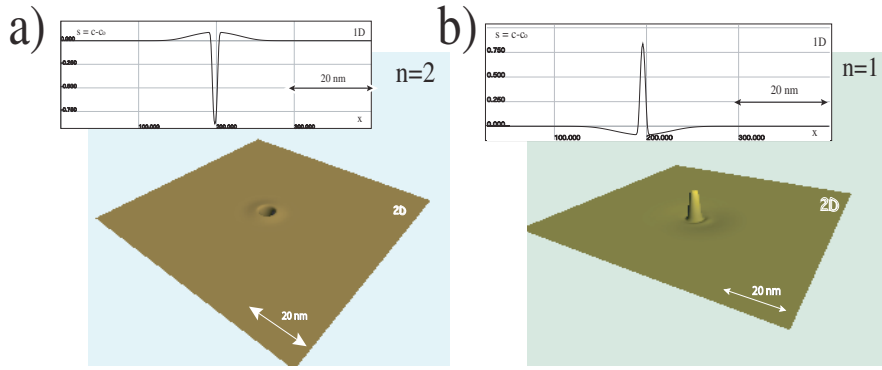

Fig. 12. Numerical simulations of equation (5) in the regime of perturbed C.H equation in one and two dimensional system. a) Vacancy island: nano localized pattern obtains from model (5), for: $n = 2, c_o = 0.9009, \alpha_o = 0.00409, \beta_o = 0.0005, \gamma = 1$, and $\mu = 0.1$. the extreme values of coverage are $\sigma_{max} = 0.0087, \sigma_{min} = -0.87$ and $\sigma \equiv c - c_o$. b) Adsorption island: Nano-localized pattern obtains from model (5), for: $n = 1$, $c_o = 0.1, \mu = 0.105, \alpha_o = 0.0005$, and $\beta_o = 0.0045$. The extreme values of coverage are $\sigma_{min} = -0.0852$, and $\sigma_{max} = 0.83814$, and $\sigma \equiv c - c_o$.

localized structures. Hence, in this extreme limit the localized coverage state are consequence of a size effect. In the case of $\{A, B\} \ll C \ll 1$, we observe numerically only desorption island solutions as the analytical result shows. We have checked the variation of the size of the adsorption and desorption island as function of the system size. Hence, the nano-localized coverage state are a robust phenomena in the covering dynamics, when the system has two ingredients: local kinetic processes and non Fickian transport as stated in the introduction.

In order to estimate the spatial size of patterns and localized structures, we can consider the typical values of the Al deposited on $TiN(100)$; at room temperature the lattice constant is $a_{Al} = 4.05 \times 10^{-10}$m, the pair interaction energy $\varepsilon = -0.22\,\text{eV}$ the lattice coordination number $\gamma = 4(\varepsilon_o = \gamma\varepsilon$ and $\zeta_o = \gamma\,\varepsilon a^2)$ and molecular dynamics simulations give the diffusion coefficient $D = K_B T M = 10^{-10}\,\text{cm}^2\,\text{s}^{-1}$. Hence, the spatial size of patterns and localized structures is of the order of 30 nm, and 8 nm for the localized structures of the bubble type, and these localized structures are *Nano Localized patterns*. It is important to notice that experimentally vacancy islands of the order of the nanometer have been observed in an absorbed mono-atomic layer of Ag deposited at room temperature on $Ru(0001)$ [8].

6 Discussion and conclusions

We have studied the coverage dynamics of a mono layer on a substrate, where the main ingredients are the local kinetics process like absorption and desorption processes and the nonlinear transport induced by atom-substrate-atom interactions. This mesoscopic approach is interesting, since it is able to modelize the growth of thin-films of large sizes, and this is what we have done in this paper. We have shown that reaction diffusion models, with transport processes leading to non Fickian diffusion, turn out to be a suitable description which allows us to understand the complex coverage dynamics. Below a critical temperature T_p and different parameters range, the non-Fickian diffusion terms are responsible of a spatial instability that give rise to the appearance of patterns coverage state, that is, the system exhibits spatially an alternation of high and small coverage. Different local kinetics processes have been consider (linear and nonlinear) and patterns coverage state persist. Hence, this dynamical behavior is a robust phenomenon in coverage dynamics. The effect of the pattern formation in the crystal growth, i.e. the effect of pattern formation over the other layer, is an open question and work in this direction is in progress.

Numerically, we observe that the pattern coverage state can coexist with the uniform cover age one, then localized coverage structures are expected. These type of state are a consequence

of the appearance of nucleation barriers between the pattern and uniform coverage states, i.e. the pinning mechanism. For different parameters range of the coverage model, we have found the robust behavior of these structures. Analytically, we have find an amplitude equation for nano localized pattern formation in the nonlinear desorption case, and numerically pattern and nano localized structure formation and bistablity of pattern solutions in both the $n = 1$ and $n = 2$ cases. We have found besides the typical width of these localized structures in the case when we can approximate the equation as a perturbed Cahn Hilliard model. Therefore, the nanolocalized solutions are a robust phenomena in the coverage dynamics, when the system has two ingredients: local kinetic processes and non Fickian transport as stated in the introduction. The localized coverage structures can exhibit complex dynamics, preliminary numerical simulations show that these states have repulsive interaction between them, work in this direction is in progress.

The system also has coexistence between two pattern coverage states, in this parameter region the system exhibits big localized patterns (localized peaks), that is, a localized pattern state surrounded by another pattern state.

The simulation software *DimX* developed at the INLN laboratory in France has been used for the numerical simulations. M.G.C. and E.T acknowledges the support of FONDAP grant 1020374 and *Programa Bicentenario Anillo* grant ACT15.

A Derivation of equation (3)

We shall give a short derivation of our starting equation (2). We divide the surface of deposition in cells of volume $V = a^d$ where d is the dimension (here $d = 1$ or $d = 2$), where the length a is smaller than the characteristic lengths of variation of the concentration $c(\vec{r}, t)$ of the adsorbed molecules and of the range of interaction between them. Following the approach and notations in [30], we assume complete diffusional *mixing* in each cell and call $N_{\vec{r}}$ the number of adsorbed molecules in the cell of position $\vec{r}$, and $\vec{r} \pm \vec{a}_i$, $\vec{a}_i = a\hat{e}_i$ $i = 1, 2 \ldots d$, are the position vectors of the $2d$ neighboring cells ($|\vec{a}_i| = a$), with $\hat{e}_1, \hat{e}_2, \ldots, \hat{e}_d$) an orthonormal basis. We shall write a multivariate master equation for the probability $p[\{N_{\vec{r}}\}, t]$ of having $N_{\vec{r}}$ molecules in cell $\vec{r}$ at time t considering two type of contributions: i) Local processes in each cell such as adsorption and desorption of the molecules which are in a gaseous state and in thermodynamic equilibrium over the substrate; ii) Transport processes between the different neighboring cells. In i) let N be the maximum number of available sites for deposition in each cell. The probabilities per unit time of an absorption or a desorption will be proportional to the number of empty sites and the number of occupied sites in each cell, respectively, and can be written as $\bar{\omega}^a(N_{\vec{r}}) = \omega^a(N - N_{\vec{r}})$, $\bar{\omega}^d(N_{\vec{r}}) = \omega^d N_{\vec{r}}$, where the probabilities of absorption an desorption for one particle in one site correspond to $\omega^a = K_a P_s, \omega^d = k_{d,o} \exp(\beta U(\vec{r}))$, $\beta = k_B T$, with $k_{d,o}$ the desorption rate and k_a the absorption rate of one molecule in an isolated site, P the pressure of the thermal bath, s is the sticking coefficient, $U(\vec{r})$ the interaction potential induced in cell $\vec{r}$ by the other adsorbed molecules, T the temperature and k_B Boltzmann constant.

We define the operators $E^{\pm 1}_{\vec{r}} - \exp(\pm \frac{1}{N} \frac{\partial}{\partial c_{\vec{r}}})$, $c_{\vec{r}} = N_{\vec{r}}/N$, and we take the probabilities per unit time of transition to neighboring cells with a Metropolis algorithm as $\tilde{\omega}_{\vec{r}\vec{r}_{\pm}\vec{a}_i} = \omega_{\vec{r} - \vec{r} \pm \vec{a}_i}(\frac{N - N_{\vec{r} \pm \vec{a}_i}}{N}) N_{\vec{r}}$ with

$$\omega_{\vec{r} \to \vec{r} \pm \vec{a}_i} = \begin{cases} v e^{U(\vec{r}) - U(\vec{r} \pm \vec{a}_i)} & U(\vec{r}) < U(\vec{r} \pm \vec{a}_i) \\ v, & U(\vec{r}) < U(\vec{r} \pm \vec{a}_i) \end{cases}$$

where v is the rate of transition between cells in the absence of interaction. The master equation can now be written as

$$\partial_t P[\{c_{\vec{r}}\}, t] = I + \sum_{i=1}^{d} II,$$

where $II_i = II(+\vec{a}_i) + II(-\vec{a}_i)$,

$$I = \sum \vec{r}\left[(E_{\vec{r}}^{-1} - 1)\omega^a N(1 - c_{\vec{r}}) + (E_{\vec{r}}^{+1} - 1)\omega^d(\vec{r})Nc_{\vec{r}}\right]p[\{c_{\vec{r}}\}, t],$$
$$II(\pm\vec{a}_i) = \sum_{i=1}^{d} \sum \vec{r}(E_{\vec{r}}^{+1}E_{\vec{r}+\vec{a}_i}^{-1} - 1)\omega_{\vec{r}\vec{r}\pm\vec{a}_i} Nc_{\vec{r}}(1 - \vec{r} \pm \vec{a}_i)p[\{c_{\vec{r}}\}, t].$$

In the equation for $\partial_t p$ the term I represents the local processes inside each cell and II_i the transport contributions. We define the density of sites per unit volume $\mu = N/V$, and the quantities (in the continuum limit $a \to 0$)

$$\begin{aligned}
\sigma_i(\vec{r}) &= \frac{\omega_{\vec{r}\to\vec{r}+\vec{a}_i} + \omega_{\vec{r}\to\vec{r}-\vec{a}_i}}{2} \\
&= \frac{v}{2}\left[1 + \exp\left(-\alpha\beta\left|\frac{\partial U}{\partial x_i}\right|\right)\right], \\
\gamma_i(\vec{r}) &= \frac{\omega_{\vec{r}\to\vec{r}+\vec{a}_i} + \omega_{\vec{r}\to\vec{r}-\vec{a}_i}}{2} \\
&= -\frac{v}{2}\left[1 - \exp\left(-a\beta\left|\frac{\partial U}{\partial x_i}\right|\right)\right] sign\left(\frac{\partial U}{\partial x_i}\right).
\end{aligned}$$

We can write $E_{\vec{r}}^{+1}E_{\vec{r}\pm\vec{a}_i}^{-1} = \exp[\frac{1}{\mu V}\sum'_{\vec{r}}(\delta_{\vec{r},\vec{r}'} - \delta_{\vec{r}\pm\vec{a}_i,\vec{r}'})\frac{\partial}{\partial c_{\vec{r}'}}]$. In the continuum limit we have

$$\frac{1}{V}\delta_{\vec{r},\vec{r}'}\delta^{(d)}(\vec{r} - \vec{r}'); \qquad \frac{1}{V}\frac{\partial}{\partial c_{\vec{r}}} \to \frac{\delta}{\delta c(\vec{r})},$$

and developing the exponentials we can write

$$\begin{aligned}
II(\pm\vec{a}_i) = \mu V \sum_{\vec{r}} &\left[\sum_{l\geq 1} \frac{1}{l!}\frac{1}{\mu^l}\int \prod_{k=1}^{l} d\vec{r}_k \prod_{k=1}^{l}(\delta(\vec{r} - \vec{r}_k) - \delta(\vec{r} \pm \vec{a}_i - \vec{r}_k))\frac{\delta}{\delta c(\vec{r}_k)}\right] \\
&\times \omega_{\vec{r}\,\vec{r}\pm\vec{a}_i} c(\vec{r})(1 - c(\vec{r} \pm \vec{a}_i)p[\{c_{\vec{r}}\}, t].
\end{aligned}$$

From the previous formula we can expand $II_i = II(+\vec{a}_i) + II(-\vec{a}_i) = \sum_{l=l}^{l=\infty} II_i^{[l]}$ where l counts the number of functional derivatives in each term of the expansion. Furthermore we expand in powers of the small size a of the cells each $II_i^{[l]} = II_i^{[l](a^2)} + II_i^{[l](a^2)} + \ldots$ For the reaction part I in each cell we expand also the exponentials and we write $I = I^{[1]} + I^{[2]} + \ldots$ We shall take only the previous terms in the master equation which is a consistent Fokker-Planck approximation. Then our equation will be

$$\partial_t p[\{c_{\vec{r}}\}, t] = I^{[1]} + I^{[2]} + \sum_{i=1}^{d}\left[II_i^{[1](a)} + II_i^{[1](a^2)} + II_i^{[2](a^2)}\right].$$

In the the continuous limit $a \to 0$ we shall have (we assume that in the limit $a^2 v$ remains finite and is equal to the diffusion constant)

$$\lim_{a\to 0} a^2\sigma_i(\vec{r}) = \lim_{a\to 0}\frac{a^2 v}{2}(1 + 1 + O(a)) = a^2 v = D$$
$$\lim a\gamma_i(\vec{r}) = \lim_{a\to 0} -\frac{av}{2}\left(-a\beta\left|\frac{\partial U}{\partial x_i}\right|\right) sign\left(\left|\frac{\partial U}{\partial x_i}\right|\right) = \frac{D\beta}{2}\frac{\partial U(\vec{r})}{\partial x_i},$$

and we can finally write the equation for $\partial_t p$ when $a \to 0$ and in space dimension $d = 2$ (orders μ^0 and μ^-1)

$$\begin{aligned}\partial_t p[\{c(\vec{r})\},t] = \int d\vec{r}\frac{\delta}{\delta c(\vec{r})}\Big[&-\omega^a(1-c(\vec{r})) + k_{d,o}e^{\beta U(\vec{r})}c(\vec{r})\\ &-D\{\nabla^2 c(\vec{r})(1-c(\vec{r}) + c(\vec{r})\nabla^2 c(\vec{r})\}\\ &-\beta D\partial_i\{c(\vec{r})(1-c(\vec{r}))\partial_i U(\vec{r})\}p[\{c(\vec{r})\},t\Big]\\ &+\frac{1}{2\mu}\int d\vec{r}\Big[\Big[\frac{\delta^2}{\delta c(\vec{r})^2}\Big[\omega^a(1-c(\vec{r})) + k_{d,o}e^{\beta U(\vec{r})}\Big]\\ &+\partial_i\frac{\delta}{\delta c(\vec{r})}\partial_i\frac{\delta}{\delta c(\vec{r})}2Dc(\vec{r})(1-c(\vec{r}))\Big]\,p[\{c(\vec{r})\},t\Big].\end{aligned}$$

This is a functional Fokker-Planck equation which is equivalent to a Langevin equation which we can write unambiguously [31], since the stochastic part is completely characterized. One has

$$\begin{aligned}\partial_t c(\vec{r},t) = R(c(\vec{r},t)) + \vec{\nabla}\cdot(D\vec{\nabla}c(\vec{r},t) + \beta Dc(1-c)\vec{\nabla}U(\vec{r})) + \Big\{&\frac{1}{\mu^{\frac{1}{2}}}[k_a P(1-c(\vec{r},t))]^{\frac{1}{2}} f_a(\vec{r},t)\\ &+ (k_{d,o})^{\frac{1}{2}} e^{\frac{1}{2}\beta U(\vec{r})} f_d(\vec{r},t) + \partial_i([2Dc(1-c)]^{\frac{1}{2}} f^i(\vec{r},t)\Big\}.\end{aligned}$$

The term $R(c(\vec{r},t))$ represents the local processes which occur in each cell and the terms proportional to D are the transport between the cells. The other terms are stochastic and order $1/\mu^{1/2}$ where $(f_a,\, f_d, f^i, i = 1,2)$ are gaussian white noises of zero mean and correlation $\langle f_a(\vec{r},t)f_a(\vec{r}_1,t_1)\rangle = \delta(\vec{r}-\vec{r}_1)\delta(t-t_1, \langle f_d(\vec{r}_1,t_1)\rangle = \delta(\vec{r}-\vec{r}_1)\delta(t-t_1)$, $\left\langle f^i(\vec{r},t)f^j(\vec{r}_1,t_1)\right\rangle = \delta_{ij}\delta(\vec{r}-\vec{r}_1)\delta(t-t_1), i,j = 1,2$. Putting $\alpha_o = \omega^a, \beta_o = \omega^d$, the term $R(c(\vec{r},t))$ takes the form

$$R(c(\vec{r},t)) = \alpha_o(1-c) + \beta_o c^n, \quad n = 1,2$$

In our derivation here we consider linear desorption which corresponds to $n = 1$, which was introduced in the first paragraph of this Appendix when we wrote $\bar{\omega}^d(N_{\vec{r}}) = \omega^d N_{\vec{r}}$ for the local desorption term in the master equation (in cell $\vec{r}$). There are however processing methods such as sputtering and laser assisted deposition (non-equilibrium processes) where we have nonlinear desorption which corresponds to $n = 2$ in the previous equation. The equations that we have consider in our study is the deterministic part of the Langevin type equations written above.

References

1. T. Zambelli, J. Trost, J. Wintterlin, G. Ertl, Phys. Rev. Lett. **76**, 795 (1996)
2. V. Gorodestkii, J. Lauterbach, H.A. Rotermund, J.H. Block, G. Ertl, Nature **370**, 276 (1994)
3. K. Kern, H. Niehus, A. Schatz, P. Zeppenfeld, J. Goerge, G. Comsa, Phys. Rev. Lett. **67**, 855 (1991)
4. T.M. Parker, L.K. Wilson, N.G. Condon, F.M. Leibsle, Phys. Rev. B **56**, 6458 (1997)
5. H.Brune, M. Giovannini, K. Bromann, K. Kern, Nature **394**, 451 (1998)
6. H. Röder, R. Schuster, H. Brune, K. Kern, Phys. Rev. lett. **71**, 2086 (1993)
7. P.G. Clark, C.M. Friend, J. Chem. Phys. **111**, 6991 (1999)
8. K. Pohl, M.C. Bartelt, J. de la Figuera, N.C. Bartelt, J. Hrbek, R.Q. Hwang, Nature **397**, 238 (1999)
9. T.S Cale, V. Mahadev, *Modeling of Film Deposition for Microelectronic-Applications*, Vol. 22, (Academic Press, New York, 1996), p. 175
10. A.S. Mikhailov, M. Hildebrand, J. Phys. Chem. **100**, 19089 (1996)
11. J. Verdasca, G. Dewel, P. Borckmans, Phys. Rev. E. **55**, 4828 (1997)

12. D. Waelgraf, Phil. Mag. **83**, 3829 (2003)
13. M.G. Clerc, M. Trejo, E. Tirapegui, Phys. Rev. Lett. **97**, 176102 (2006)
14. D. Waelgraf, Physica E **15**, 33 (2002)
15. M. Hildebrand, A.S. Mikhailov, G. Ertl, Phys. Rev. E **58**, 5483 (1998)
16. M.G. Clerc, C. Falcon, Physica A **356**, 48 (2005)
17. P. Coullet, C. Riera, C. Tresser, Rev. Lett. **84**, 3069 (2002)
18. C. Elphick, E. Tirapegui, M. Brachet, P. Coullet, G. Iooss , Physica D **29**, 95 (1987)
19. D. Bensimon, B. I. Sharaiman, V. Croquette, Phys. Rev. A **38**, 5461 (1988)
20. M.G. Clerc, C. Falcon, E. Tirapegui, Phys. Rev. Let. **94**, 148302 (2005)
21. M.G. Clerc, C. Falcon, E. Tirapegui, Phys. Rev. E **74**, 011303 (2006)
22. U. Bortolozo, M.G. Clerc, C. Falcon, S. Residori, R. Rojas, Phys. Rev. Lett. **96**, 214501 (2006)
23. H. Calisto, M. Clerc, R. Rojas, E. Tirapegui, Phys. Rev. Lett. **85**, 3805 (2000); M. Argentina, M.G. Clerc, R. Rojas, E. Tirapegui, Phys. Rev. E **71**, 046210 (2005)
24. J.W. Cahn, J.E. Hilliard, J. Chem. Phys. **31**, 688 (1959)
25. C. Chevallard, M. Clerc, P. Coullet, J.M. Gilli, Eur. Phys. J. E **1**, 179 (2000)
26. C. Chevallard, M. Clerc, P. Coullet, J.M. Gilli, Europhys. Lett. **58**, 686 (2002)
27. H. Calisto, M. Clerc, R. Rojas, E. Tirapegui, Phys. Rev. Lett. **85**, 3805 (2000)
28. M. Argentina, M.G. Clerc, R. Rojas, E. Tirapegui, Phys. Rev. E **71**, 046210 (2005)
29. M.C. Cross, P.C. Hohenberg, Rev. Mod. Phys. **65**, 851 (1993)
30. F. Langouche, D. Roekaerts, E. Tirapegui, Phys. Lett. A **82**, 309 (1981)
31. F. Langouche, D. Roekaerts, E. Tirapegui, *Functional Integration and Semiclassical Expansions* (Reidel, 1982)